Even illumination in total internal reflection fluorescence microscopy using laser light

ARTICLE *in* MICROSCOPY RESEARCH AND TECHNIQUE · JANUARY 2008

Impact Factor: 1.15 · DOI: 10.1002/jemt.20527 · Source: PubMed

4 AUTHORS, INCLUDING:

Reto Fiolka
University of Texas Southwestern Medical Ce…
20 PUBLICATIONS **359** CITATIONS
SEE PROFILE

Helge Ewers
Freie Universität Berlin
34 PUBLICATIONS **1,079** CITATIONS
SEE PROFILE

Even Illumination in Total Internal Reflection Fluorescence Microscopy Using Laser Light

R. FIOLKA,[1] Y. BELYAEV,[1] H. EWERS,[2] AND A. STEMMER[1]*
[1]*Nanotechnology Group, ETH Zurich, Tannenstrasse 3, CH-8092 Zurich, Switzerland*
[2]*Institute of Biochemistry, ETH Zurich, Schafmattstr. 18, CH-8093 Zurich, Switzerland*

KEY WORDS total internal reflection fluorescence (TIRF) microscopy; evanescent fields; illumination; intereference fringes; coherence

ABSTRACT In modern fluorescence microscopy, lasers are a widely used source of light, both for imaging in total internal reflection and epi-illumination modes. In wide-field imaging, scattering of highly coherent laser light due to imperfections in the light path typically leads to nonuniform illumination of the specimen, compromising image analysis. We report the design and construction of an objective-launch total internal reflection fluorescence microscopy system with excellent evenness of specimen illumination achieved by azimuthal rotation of the incoming illuminating laser beam. The system allows quick and precise changes of the incidence angle of the laser beam and thus can also be used in an epifluorescence mode. *Microsc. Res. Tech. 00:000–000, 2007.*

INTRODUCTION

Over the past 2 decades, total internal reflection fluorescence (TIRF) microscopy has become a method of choice for cell biologists (Axelrod, 2003; Schneckenburger, 2005). TIRF allows one to specifically excite fluorescent molecules within a narrow layer adjacent to the cover slip. By now this method has found numerous applications in studies of protein trafficking, membrane dynamics, endocytosis, exocytosis, and virus movement (Aravanis et al., 2003; Pelkmans and Zerial, 2005; Pelkmans et al., 2001; Smith et al., 2004; Steyer and Almers, 1999; Toomre et al., 2000), to name just a few examples.

The foundation of TIRF is based on the effect called total internal reflection (TIR); at the interface of two media with different refractive indices n_1 and n_2, light traveling within the denser medium (with index n_1) experiences TIR when approaching the interface at incident angles higher than the so called critical angle $\alpha_c = arcsin\,(n_2/n_1)$. In the less dense medium, the light forms a so called evanescent field. The penetration depth d of the evanescent field depends on the wavelength of the incident light, the ratio of the refractive indices, and the incidence angle α as follows:

$$d = \lambda/(4\pi \cdot n_2)\left(\sin^2\alpha - \sin^2\alpha_c\right)^{-1/2} \qquad (1)$$

Currently, lasers are routinely used light sources in TIRF microscopy. In wide-field systems, however, the advantage of high brilliance and good beam collimation is compromised by uneven specimen illumination caused by interference fringes due to scattering of the highly coherent laser light at nonuniformities in the light path. Additionally, anisotropic blur occurs when the evanescent field is perturbed by a mismatch in refractive index between the specimen and the surrounding media (Mattheyses and Axelrod, 2006). Such illumination conditions severely hamper quantitative image analysis. A system ensuring even specimen illumination would greatly facilitate this task.

Recently, a promising method to improve the quality of laser illumination in a TIRF setup has been reported (Mattheyses and Axelrod, 2005), where the illuminating laser beam is azimuthally spun by means of a rotating glass wedge. Thereby, interference fringes and anisotropic blur are averaged out and a uniform illumination results. However, this setup does not allow one to easily change the incident angle, which is essential to control the penetration depth d and to apply techniques like multi-angle evanescent wave microscopy (Rohrbach, 2000) or variable-angle TIRF microscopy (Stock et al., 2003).

Here we report on the design and performance of a TIR-illumination system that employs azimuthal rotation of the incoming laser beam and enables fast changing of the incident angle. This setup yields an excellent evenness of the excitation field and precise control over the penetration depth of the evanescent wave. Furthermore, switching between TIRF and a hollow-cone epifluorescence mode is feasible.

We investigate the system performance by comparing images of HeLa cells acquired using either unidirectional or azimuthally rotated laser beams. These measurements are complemented by an analysis of the corresponding illumination intensity profiles acquired from thin layers of aqueous fluorescein solution. Control over the penetration depth of the excitation field is demonstrated on fluorescent microspheres embedded in agarose.

*Correspondence to: A. Stemmer, Nanotechnology Group, ETH Zurich, Tannenstrasse 3, CH-8092 Zurich, Switzerland. E-mail: astemmer@ethz.ch

Present address of Y. Belyaev: Advanced Light Microscopy Facility, European Molecular Biology Laboratory, Meyerhofstr. 1, 69117 Heidelberg, Germany.

Received 9 March 2007; accepted in revised form 29 June 2007

DOI 10.1002/jemt.20527

Published online in Wiley InterScience (www.interscience.wiley.com).

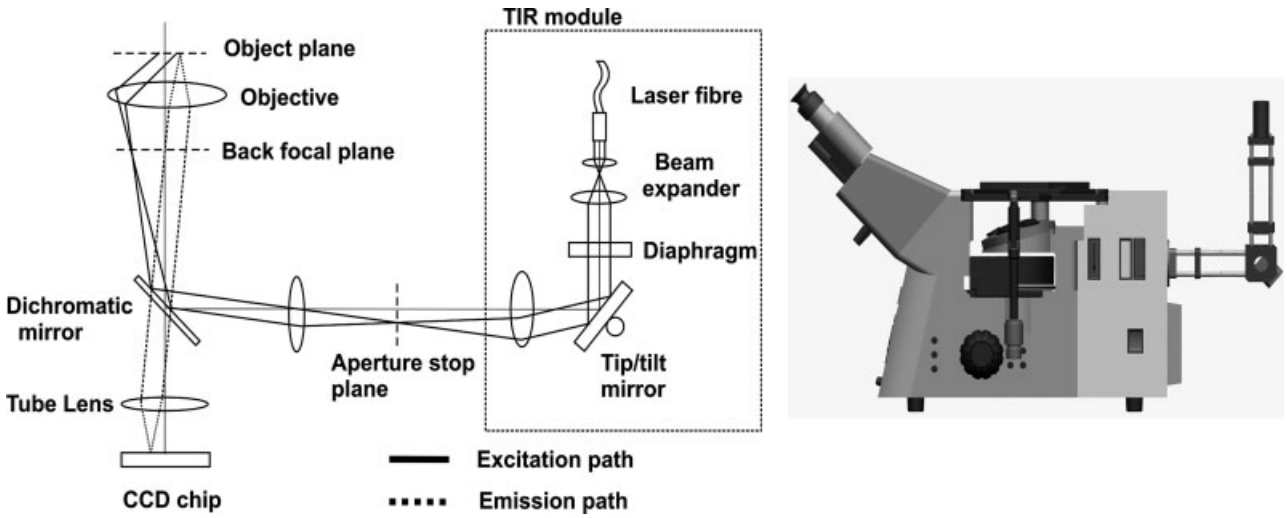

Fig. 1. Optical train of the illumination system. A two axes tip/tilt mirror spins a focused laser beam azimuthally in the back focal plane of the objective. The incident angle of the laser beam is controlled by the same mirror. The inset on the right shows a model of the microscope system.

MATERIALS AND METHODS

Optical Set Up

The illumination system employs an objective-launch TIRF setup (Axelrod, 2001). A collimated laser beam is coupled into the standard epi-illumination beam path at the lamp port and is focused on the back focal plane (BFP) of the objective lens (Fig. 1). Consequently, a collimated laser beam emerges from the objective. The angle of incidence and the azimuthal angle of the emerging beam are controlled by steering the focal spot in the BFP by a two axes tip/tilt mirror.

To illuminate a sufficiently large area of the specimen, the laser beam emerging from an optical fiber (beam waist diameter 1 mm) is expanded five times. An iris diaphragm placed behind the beam expander allows one to adjust the size of the illuminated specimen area.

Azimuthal rotation of the specimen illumination is achieved by moving the focal spot on a circular trajectory in the BFP, as introduced by Ellis (Ellis, 1988) for phase contrast and Axelrod for TIRF (Mattheyses and Axelrod, 2005) microscopy. The angle of incidence is controlled by adjusting the radius of the circular trajectory.

Trans-illumination results when the incident angle is smaller than the critical angle. Combined with azimuthal rotation, the time averaged excitation field forms a hollow cone, whereas in standard epifluorescence, the excitation field is a stationary full cone. In principle, it would be possible to quickly scan the whole BFP to obtain a time averaged full cone. As we will demonstrate below, the hollow cone creates an excitation field suitable for epifluorescence imaging.

The experimental set up was realized on a Zeiss Axiovert 200M inverted microscope as shown in the inset in Figure 1. No further modifications of the microscope were necessary.

A Zeiss α Plan-Fluar 100×, NA 1.45 oil immersion objective was used for the TIR experiments. Digital images were acquired using a cooled CCD camera with FireWire connection (ORCA ER, Hamamatsu, Japan). A LabView program controlled the microscope settings, the image acquisition and the tip/tilt mirror. For image acquisition, the frame rate of the camera was synchronized to the rotation speed of the illumination field to ensure whole numbers of completed azimuthal rotations. The tip/tilt mirrors were run at 20 Hz and typical integration times were 200–500 ms. The laser power of the beam emanating from the objective was set to 0.1–0.6 mW, unless stated differently.

Sample Preparation

HeLa cells stably transfected with actin-GFP were grown on coverslips. Fluorescent microspheres of 200 nm diameter (Polyscience, Warrington, PA) were mixed 1:1,000 with 1% Agarose (Sigma-Aldrich, St. Louis, MO) and small drops of this mixture were sandwiched between a glass slide and a coverslip. Fluorescein (Polyscience, Warrington, PA) was mixed with UHQ water in a ratio of 1 μg/mL and small drops were put on a coverslip. To probe the penetration depth of the evanescent field a test specimen was fabricated as follows. Fluorescent microspheres of 50 nm diameter (Polyscience, Warrington, PA) were mixed 1:10,000 with UHQ water and small drops were dried on a coverslip. This coverslip was mounted upside down on a second one using two layers of double sided tape at one edge to form a gentle slope. The wedge-shaped space between the two coverslips was filled with UHQ water.

RESULTS

In Figure 2, the actin cytoskeleton of a HeLa cell (maximum thickness about 10 μm) is imaged using either unidirectional or azimuthal rotation TIRF microscopy at the same incident angle. In Figure 2a, anisotropic blur orientated parallel to the unidirectional illumination beam is evident. This directional artifact

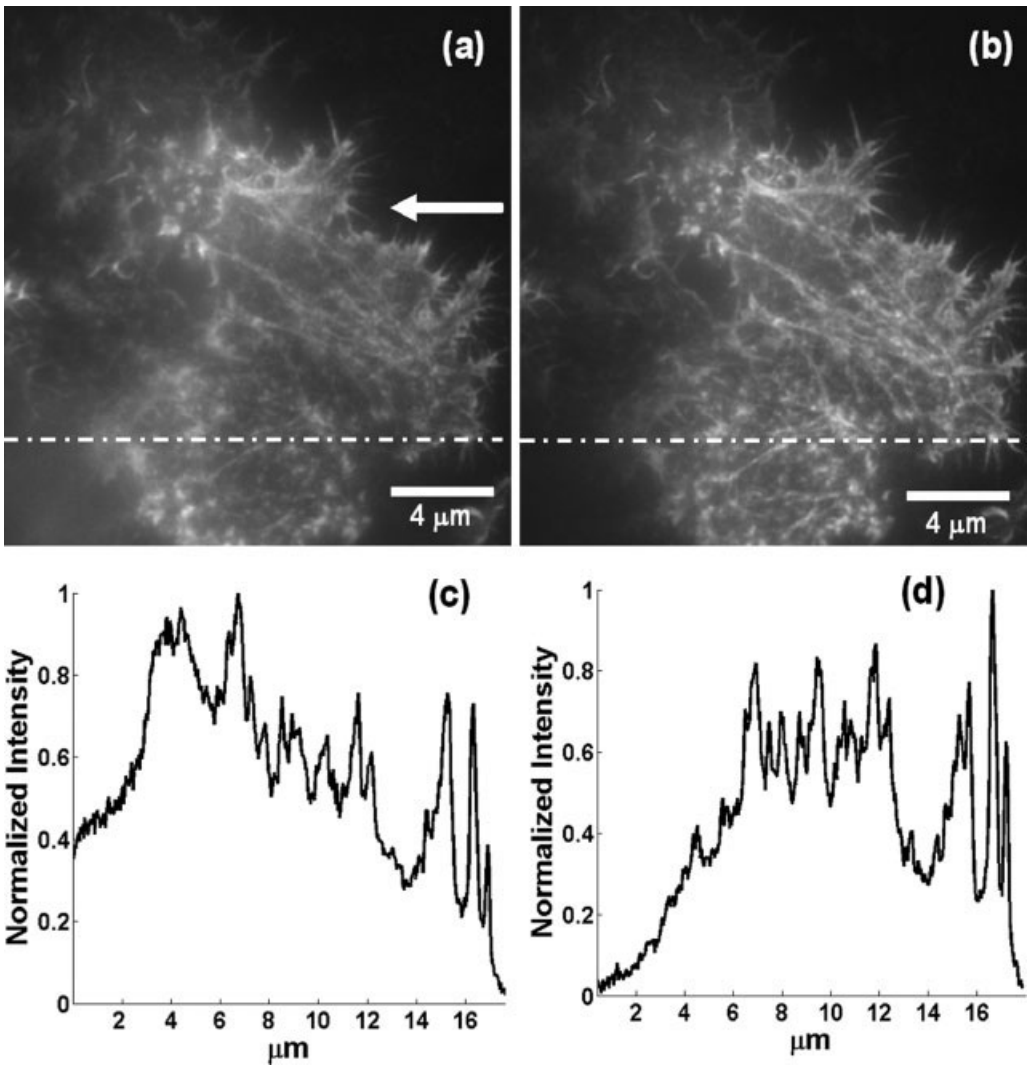

Fig. 2. The actin cytoskeleton of a HeLa Cell imaged with (**a**) conventional and (**b**) azimuthal rotation TIRF microscopy. The arrow in figure (a) indicates the propagation direction of the excitation laser beam. Corresponding cross sections are shown in (**c**) and (**d**).

is clearly averaged out in the image shown in Figure 2b, which is acquired using azimuthal rotation. Cross sections of the corresponding images show a ramp-like increase of intensity for unidirectional TIR illumination (Fig. 2c), whereas in the case of rotating illumination, the intensity distribution is more uniform (Fig. 2d).

In Figures 3a and 3b, we compare the performance of unidirectional and azimuthal rotation TIRF microscopy on a thin (about 1 μm) HeLa cell. As the difference between the two illumination modes is minimal, we conclude that for thin specimens the perturbation of the evanescent field has no significant influence on TIRF imaging. Figure 3c shows a hollow-cone (incident angle below the critical angle) epifluorescence image of the cell at the same focal level.

The possibility to vary the incident angle is illustrated in Figure 4 for a group of 200 nm diameter microspheres. In Figure 4a the incident angle is set to 73°, the maximum angle permitted by the numerical aperture of the objective. In Figures 4b and 4c, the incident angle is set to 67.5 and 62°, respectively. The latter value is only slightly higher than the critical angle. As the penetration depth d increases when the incident angle decreases, more and more microspheres are excited and become visible, as clearly shown in the sequence of Figures 4a–4c.

To measure the penetration depth more quantitatively, we employed a test specimen with 50-nm-diameter fluorescent microspheres attached to an inclined coverslip above the coverslip contacting the objective (Fig. 5). This set-up allows one to vary the separation between the fluorescent probes and the glass–water interface where the evanescent field is created by laterally moving the specimen. We measured intensities for epi-illumination, unidirectional TIRF, and azimuthal rotation TIRF at an incident angle of 65° and computed the corresponding penetration depths. The penetration depth for unidirectional TIRF illumination was 125 ±

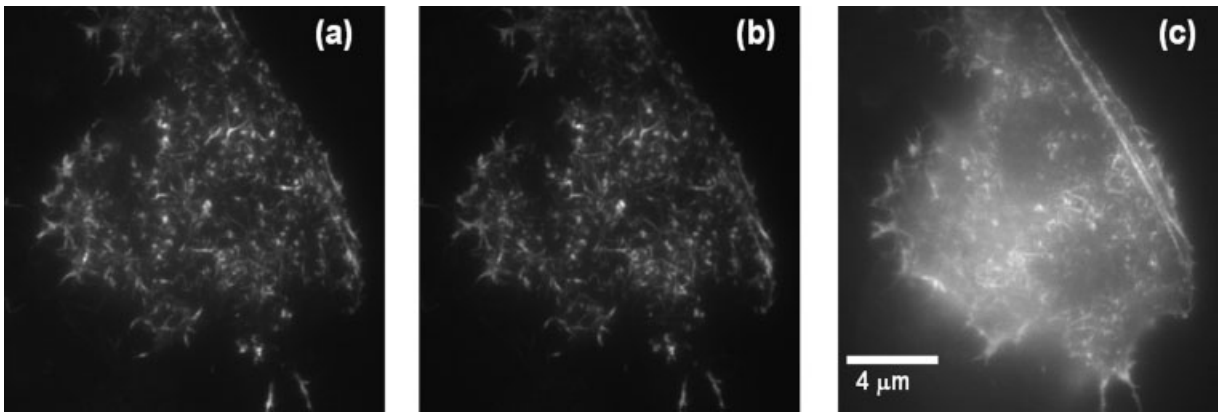

Fig. 3. Actin cytoskeleton of a thin HeLa cell imaged with: (**a**) unidirectional TIRF microscopy; (**b**) azimuthal rotation TIRF microscopy; (**c**) hollow-cone epifluorescence illumination.

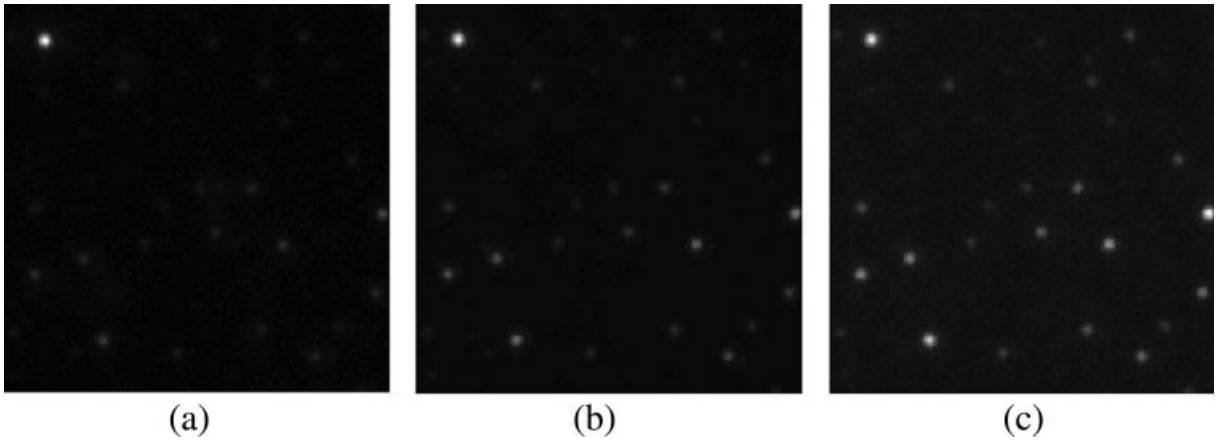

Fig. 4. A group of fluorescent microspheres with a diameter of 200 nm imaged with azimuthal rotation TIRF microscopy at different incident angles: (**a**) 73°; (**b**) 67.5°; (**c**) 62°. Image size is $20 \times 20\ \mu m^2$.

20 nm and the penetration depth for azimuthal rotation TIRF illumination was 146 ± 15 nm. The value predicted by Eq. (1) is 108 nm.

To compare the evenness of the illumination modes, a mixture of fluorescein and water is bleached with a local evanescent field created by unidirectional or azimuthal rotation TIR. We observed that a few seconds after initiating the bleaching, the intensity distribution reached a steady state because bleached fluorophores were constantly replaced by diffusion. We conclude that this bleaching procedure is ideal for comparing the evenness of the illumination.

Figure 6 shows the steady state intensity distributions for unidirectional and azimuthal rotation TIR excitation. The laser power of the incident laser beam emanating from the objective was measured to be 1.7 mW. In Figures 6a and 6c, one can clearly see strong interference fringes for unidirectional illumination whereas in Figure 6b the intensity distribution is much more isotropic because of the azimuthal rotation. The cross section in Figure 6d displays the expected inverted Gaussian intensity profile for a Gaussian laser beam.

DISCUSSION

Even specimen illumination greatly facilitates quantitative image analysis. Quite often it is possible to compensate an inhomogenous excitation field in a post processing step, yet this approach proves rather difficult in unidirectional TIRF microscopy for fundamental reasons. The fluorescent signal is proportional to the excitation field and the fluorophore distribution, provided excitation is below the saturation-intensity of the fluorophores. However, as shown in Figures 2a and 2c, significant alterations in the excitation intensity distribution may occur due to the interaction of the evanescent light with the specimen itself, because of locally varying refractive index and optical path length. Therefore, it is not possible to derive the excitation intensity distribution from a single image. In fact, it also is not possible to use calibration data obtained on a specimen with a constant fluorophore distribution, e.g., from a fluorescent monolayer, as it represents a different imaging situation resulting in a different excitation intensity distribution. Furthermore, normalization of a unidirectional TIRF image with a dataset of a

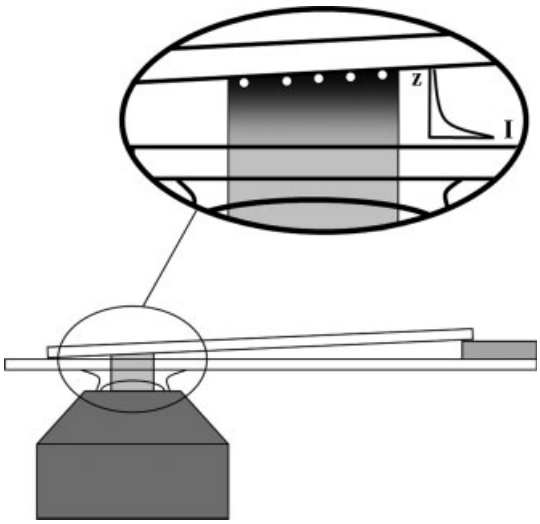

Fig. 5. Set-up for measuring the penetration depth. An evanescent field is formed at the glass water interface of the coverslip contacting the objective. The intensity of this field is probed with fluorescent microspheres attached to an inclined coverslip separated from the first one through a wedge of water.

reference excitation field may be prone to noise issues, as this procedure would require divisions by low values in regions of interference minima. Azimuthal rotation TIRF microscopy provides an elegant solution to these problems because the rotating laser beam performs rotational averaging of the specimen induced inhomogeneities in the excitation field.

An explanation for the ramp like intensity increase in Figure 2a and 2c is that evanescent photons get scattered at refractive index boundaries in the cell and are converted into propagating ones (Chew et al., 1979; Oheim and Schapper, 2005). As the photons are scattered mostly forward, the confinement of the excitation field is gradually lost in the propagation direction. As a consequence, the propagating photons excite fluorophores outside the focal plane, resulting in the observed anisotropic blur. Azimuthal rotation TIRF microscopy does not prevent light scattering in an inhomogeneous specimen, but by rotational averaging it lowers the propagation anisotropy of the forward-scattered photons. Two photon TIRF microscopy (Oheim and Schapper, 2005) can suppress the excitation of out-of-focus fluorophores by scattered light, but at the expense of high excitation intensities and more expensive laser sources.

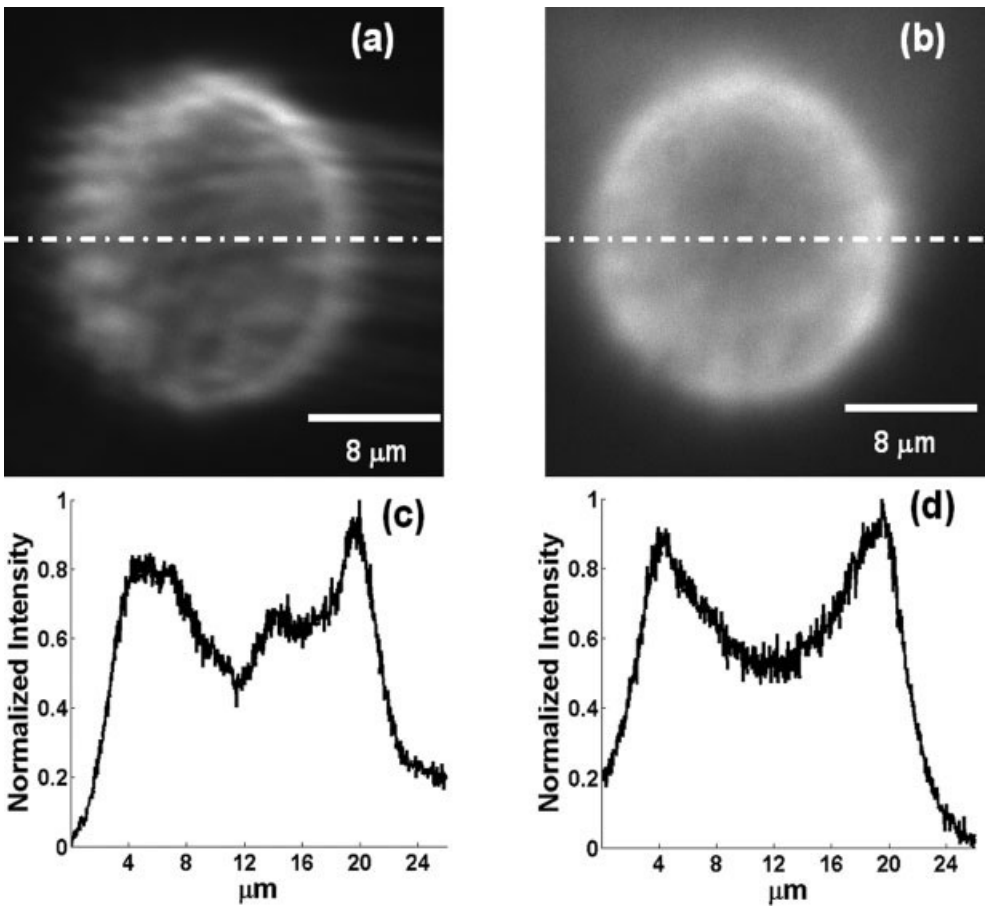

Fig. 6. Bleaching of a water/Fluorescein mixture at a laser power of 1.7 mW: (**a**) stationary intensity distribution obtained with unidirectional TIR excitation; (**b**) stationary intensity distribution obtained with azimuthal rotation TIR excitation. Corresponding cross sections of the intensity distribution are shown in (**c**) and (**d**).

The experimentally determined penetration depths agree well with the theoretical value. Nevertheless one should note that the test specimen was ideal, in the sense that the evanescent field was not perturbed by locally varying refractive indices at the glass water interface. For biological specimens, one would expect larger effective penetration depths due to the scattering phenomena described above.

The observed difference in penetration depth for unidirectional and azimuthal rotation TIRF may be due to interference fringes in the unidirectional mode and/or slight imperfections of the circular trajectory in the rotation mode. Furthermore, it is quite likely that the coverslips are not ideally flat, resulting in small changes of incident angle when the illumination is azimuthally rotated.

CONCLUSIONS

In TIRF microscopy, azimuthal spinning of the incident laser beam by means of a tip/tilt piezo mirror results in very even specimen illumination and allows one to adjust quickly the penetration depth of the evanescent field. The presented system enables fast switching between TIRF and a hollow-cone epifluorescence mode, which is very useful for correlating surface and inner structures of a specimen.

For thin specimens, the differences between azimuthal and unidirectional TIRF microscopy are minimal. For thick cells, however, images acquired with azimuthal rotation TIRF microscopy contain dramatically less blur. Interference fringes, typical for stationary laser illumination, are eliminated upon rotation and a striking evenness of the excitation field compared with conventional TIR-excitation is observed.

Providing even illumination, we expect our system to become a valuable tool for quantitative TIRF microscopy in cell biology.

ACKNOWLEDGMENTS

We would like to thank our colleagues Dr. Stefan Lengweiler for his helpful assistance in designing and constructing the system, and Dr. Andreas Vonderheit for providing cell specimens. We also thank Dr. Stefan Ballmer, Carl Zeiss Switzerland, for lending equipment and useful suggestions.

REFERENCES

Aravanis AM, Pyle JL, Tsien RW. 2003. Single synaptic vesicles fusing transiently and successively without loss of identity. Nature 423:643–647.

Axelrod D. 2001. Total internal reflection fluorescence microscopy in cell biology. Traffic 2:764–774.

Axelrod D. 2003. Total internal reflection fluorescence microscopy in cell biology. Biophotonics, Part B. San Diego: Academic Press. pp.1–33.

Chew HW, Wang D-S, Kerker M. 1979. Elastic scattering of evanescent electromagnetic waves. Appl Opt 18:2679–2687.

Ellis GW. 1988. An annular scan phase-contrast scanned aperture microscope (Aspsam). Cell Motil Cytoskeleton 10:342.

Mattheyses AL, Axelrod D. 2005. Effective elimination of laser interference fringing in fluorescence microscopy by spinning azimuthal incidence angle. Biophys J 88:341A–342A.

Mattheyses AL, Axelrod D. 2006. Direct measurement of the evanescent field profile produced by objective-based total internal reflection fluorescence. J Biomed Opt 11:014006.

Oheim M, Schapper F. 2005. Non-linear evanescent-field imaging. J Phys D: Appl Phys 38:185–197.

Pelkmans L, Kartenbeck J, Helenius A. 2001. Caveolar endocytosis of simian virus 40 reveals a new two-step vesicular-transport pathway to the ER. Nat Cell Biol 3:473–483.

Pelkmans L, Zerial M. 2005. Kinase-regulated quantal assemblies and kiss-and-run recycling of caveolae. Nature 436:128–133.

Rohrbach A. 2000. Observing secretory granules with a multiangle evanescent wave microscope. Biophys J 78:2641–2654.

Schneckenburger H. 2005. Total internal reflection fluorescence microscopy: Technical innovations and novel applications. Curr Opin Biotechnol 16:13–18.

Smith AE, Ewers H, Sbalzarini I, Koumoutsakos P, Helenius A. 2004. Alternate endocytic pathways revealed by virus entry into animal cells. Mol Biol Cell 15:195A.

Steyer JA, Almers W. 1999. Tracking single secretory granules in live chromaffin cells by evanescent-field fluorescence microscopy. Biophys J 76:2262–2271.

Stock K, Sailer R, Strauss WSL, Lyttek M, Steiner R, Schneckenburger H. 2003. Variable-angle total internal reflection fluorescence microscopy (VA-TIRFM): Realization and application of a compact illumination device. J Microsc (Oxford) 211:19–29.

Toomre D, Steyer JA, Keller P, Almers W, Simons K. 2000. Fusion of constitutive membrane traffic with the cell surface observed by evanescent wave microscopy. J Cell Biol 149:33–40.